Available online at www.sciencedirect.com
ScienceDirect
Materials Science and Engineering C 27 (2007) 8 – 13
MATERIALS SCIENCE & ENGINEERING C
www.elsevier.com/locate/msec

Structure and interactions of calcite spherulites with α-chitin in the brown shrimp (*Penaeus aztecus*) shell

A. Heredia [a,d,*], M. Aguilar-Franco [f], C. Magaña [e], C. Flores [b], C. Piña [b], R. Velázquez [c], T.E. Schäffer [d], L. Bucio [e], V.A. Basiuk [a]

[a] *Instituto de Ciencias Nucleares, Departamento de Química de Radiaciones y Radioquímica, UNAM, Circuito Exterior C.U. Apdo., Postal 70-543, 04510 México, D.F., México*
[b] *Instituto de Investigaciones en Materiales, Depto de Estado Sólido, Laboratorio de Biomateriales, UNAM, Circuito Exterior C.U. S/N CP 04510 México, D.F., México*
[c] *Centro de Física Aplicada Tecnología Avanzada, UNAM, Km. 15 Carretera Querétaro-San Luis Potosí, C.P. 76230, Querétaro, Qro. México*
[d] *Physikalisches Institut and Center for Nanotechnology, Universität Münster, Gievenbecker Weg 11, 48149 Münster, Germany*
[e] *Instituto de Física, Depto de Estado Sólido, UNAM, Circuito Exterior s/n, Ciudad Universitaria Apartado Postal 20-364 01000 México D.F., México*
[f] *Instituto de Física, Depto de Fisicoquímica, UNAM, Circuito Exterior s/n, Ciudad Universitaria Apartado Postal 20-364 01000 México D.F., México*

Received 11 May 2005; received in revised form 26 October 2005; accepted 20 November 2005
Available online 9 February 2006

Abstract

White spots form in the brown shrimp (*Penaeus aztecus*, Decapoda) shell during frozen storage. The mineral formed consists of calcite incorporated into an amorphous α-chitin matrix. We studied mechanisms of interaction of amorphous α-chitin macromolecules with *hkl* crystal planes to form highly ordered structures, as well as the role of specific sites in the biopolymer, which can be related to nucleation and spheroidal crystal growth. We used low vacuum scanning electron microscopy (LVSEM), X-ray powder diffraction (XRD), atomic force microscopy (AFM), Fourier-transform infrared spectroscopy (FT-IR), and molecular mechanics modeling (MM+ method). AFM images showed fingerprint distances in the biopolymer and a highly layered structure in the crystalline material. The presence of α-chitin, with a specific spatial distribution of radicals, is thought to be responsible for nucleation and to thermodynamically stabilize ions to form the spherulite crystalline phase, which are usually oval to spherical (0.10 to 200 μm in diameter). Our models of crystal–biopolymer interaction found high affinity of CO_3^{2-} anions in the (104) crystalline plane (the main plane in calcite monocrystals) to NH– groups of the biopolymer, as well as of the C═O in the biopolymer to Ca^{2+} cations in the crystalline structure. These interactions explain the spherical growth and inhibition in some planes. The specific physicochemical interactions (docking of groups depending on their geometrical distribution) suggest that the biomineral structure is controlled by the biopolymer on a local scale. This information is useful for further design and improvement of (hybrid) materials for versatile application, from nanotechnology to biomedicine and engineering.

Keywords: Molecular modeling (MM+); LVSEM; Shrimp; Biomineralization; α-Chitin; Calcite

1. Introduction

White spots may form in the shell of many arthropoda during frozen storage [1] as in the brown shrimp (*Penaeus aztecus*). Dried white spot material has previously been shown to consist of $CaCO_3$ in the form of calcite, incorporated into a matrix of amorphous α-chitin (poly-β-(1→4)-*N*-acetylglucosamine) [2]. The exoskeletons of Crustacean are built up by chitin, proteins, and sometimes calcium salts, phosphates and carbonates. As can occur in other systems, the mineral–organic interactions can be due to high affinity of biomacromolecules to the mineral surface [3–5]. The complex hybrid (biomineral) systems are an exciting subject for material science and solid state biophysics. The reason is that biologically synthesized mineral–organic hybrids exhibit a remarkable degree of ordering and control over the nucleating crystalline structures at nanometric and

* Corresponding author. Instituto de Ciencias Nucleares, Departamento de Química de Radiaciones y Radioquímica, UNAM, Circuito Exterior C.U. Apdo., Postal 70-543, 04510 México, D.F., México.

0928-4931/$ - see front matter © 2006 Elsevier B.V. All rights reserved.
doi:10.1016/j.msec.2005.11.003

micrometric scales, whose mechanism is not well understood [6]. Of particular interest is the affinity and specificity of some regions in the macromolecules, or monomers as aminoacids and sugars, to some (*hkl*) crystal planes from some crystals. In calcite from shrimps the interaction results mainly in a well-established and organized carbonate crystalline phase [7] with spherulite morphology (oval to spherical) and about 0.5 to 200 μm in diameter [8]. Quite remarkably, spherical shape is not typical for mineral calcite, although it is possible due to inhibition of some crystalline planes through the interaction with certain molecules or ions. The main crystal morphology for calcite is rhombohedral, and the main peak in powder X-ray diffraction patterns corresponds to its (104) plane. In the rhombohedral crystal structure, the (104) plane dominates [9].

The biological nature commonly employs hybrid interactions to improve mechanical properties of the tissues [10]; *Bivalvia* shells are perhaps the best example. Hybrid interactions are believed to play the most important role here [11,12]. Nonetheless, their detailed characterization is scarce, despite the fact that description of the mineral–macromolecule interactions is a subject for extensive studies due to their importance for the synthesis of high-performance materials [13–15]. Calcium carbonate has been widely used for studying the biomimetic processes; the synthesis of calcite crystals in the presence of organic templates allows to produce crystals with specific morphologies and sizes [16].

To explain this controlled crystal synthesis, authors regard a specific geometrical distribution of functional groups in the biopolymer as the one responsible for specific interactions with the crystalline phase, as observed in other inorganic [17] and biological systems [1,15,18].

The aim of these studies is to understand how the amorphous macromolecular structures as α-chitin couple to crystalline planes to form controlled crystalline structures, as well as to know the roles of different chemical groups in the crystal–biopolymer interaction [19,20]. Performing experiments in situ at nanoscale level and under environmental conditions is possible actually by using atomic force microscopy [19,21]. Taken together with molecular modeling, it could contribute to our understanding of the phenomena underlying this molecularly controlled process.

In the present paper, we studied the spherulites by means of low vacuum scanning electron microscopy (LVSEM), X-ray powder diffraction (XRD), atomic force microscopy (AFM), Fourier-transform infrared spectroscopy (FT-IR), along molecular mechanics modeling (MM+method) of α-chitin–calcite interactions. We tried to address the question whether α-chitin structure can match calcite surface structure, to explain the origin of the spherulite morphology by inhibiting the (100), (001) and (104) planes, as well as to describe changes in the α-chitin molecular architecture when associated to the crystalline phase. Studying this sort of structures is an inevitable step for bringing new knowledge at nanoscale level and synthetic tools to other research areas, from solid state biophysics to nascent bionanotechnology.

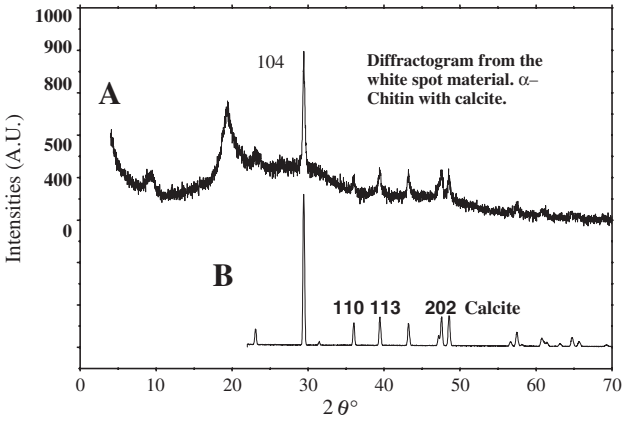

Fig. 1. X-ray diffractogram of: (A) powdered sample of the shrimp shells (white spot material) and (B) a calcite diffractogram. The contribution from amorphous solid is due to α-chitin. The highest calcite peak corresponds to (104) plane.

2. Materials and methods

Commercial dried shells of *P. aztecus* were used in the present study. Carapaces (Cephalothorax) were selected from the entire shells (containing the white material within the tissue) and washed in distilled water, without any further chemical treatment. The carapaces were cut into pieces of approximately 0.3 × 0.3 cm. Three different shells were randomly cut into pieces for analyses. To perform XRD and FT-IR analysis, the solid white material was separated by using tweezers and scalpel; an agate mortar was used for its homogenization.

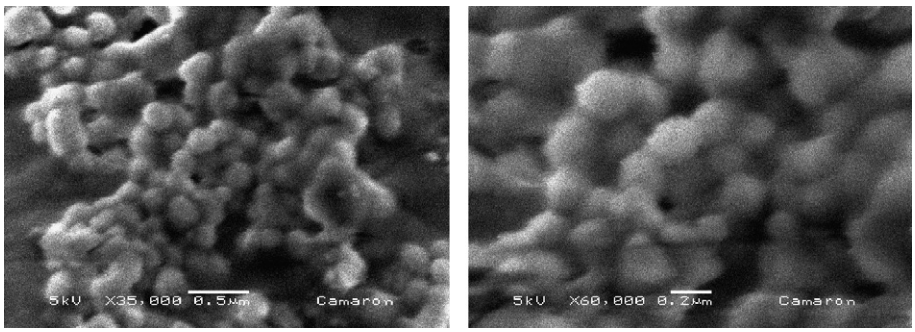

Fig. 2. Low vacuum scanning electron microscopy images of the calcite spherulites. Left, the crystalline material over amorphous α-chitin phase; right, a closer view of the spherulites. Their size is between 100 and 200 nm.

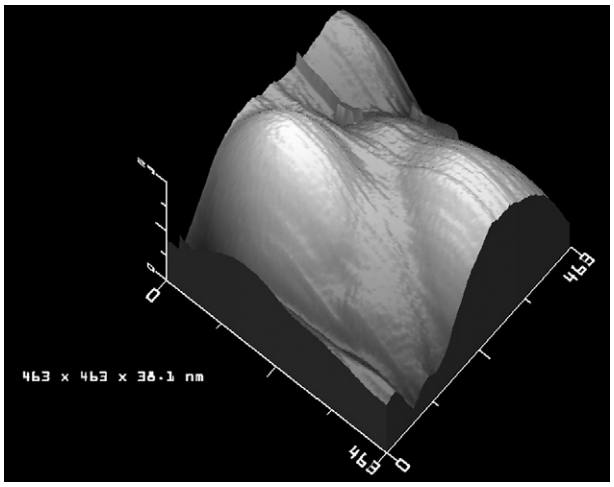

Fig. 3. AFM topography image of a shell with white spots. Scanrange: 467 × 467 nm and vertical range 38 nm.

X-ray powder diffraction was performed to identify the crystalline phase. The patterns were collected using a Siemens D5000 Diffractometer, CuKα radiation (35 kV, 25 mA), vertical goniometer fixed, graphite monochromator and scintillation counter supplied. The data were recorded using a step size of 0.5°, 5 s counting time each step (step/scan mode) over 5–110° 2θ-range.

For LVSEM observations, the sample was fixed in a sample holder using a carbon ribbon, without any additional treatment. A LVSEM JSM-5900LV instrument was used. The measurements were performed at a low vacuum of 1–250 Pa (0.01–2.5 Torr) and an acceleration voltage of 5–20 kV.

A JEOL Scanning Probe Microscope (JSPM-4210) was used for AFM studies of the shells with white spots (contact mode). A scan speed of about 215.7 nm/s was used.

To spectroscopically characterize the biopolymer–crystal interaction, FT-IR measurements were performed on a Nicolet 680 FT-IR spectrometer. The samples were ground and extracted by using tweezers and scalpel, mixed with KBr powder (100 : 1 ratio) and then compressed into pellets.

Molecular modeling was performed for calcite (100), (001) and (104) crystal planes (Trigonal, space group *R*-3 *c*, No. 167) interacting with three trimeric units of α-chitin which were made by using the crystal model and then optimized (Orthorhombic, space group $P2_12_12_1$). The crystal plane models were constructed in the CpAtoms 5.1 for Windows software (By Shape Software Inc.) and exported to HyperChem 7 (by Hypercube Inc.). The organic molecules were placed in variable positions with respect to the crystalline plane models; the geometry of the latter was frozen. For the (104) planes, two configurations, parallel and perpendicular, were used in which the α-chitin trimer chains were put in its longitudinal axis parallel or perpendicular to the calcite (010) direction. Full geometry optimization was performed with MM+ force field, Polak-Ribiere conjugate gradient algorithm and root mean square gradient of 0.005 kcal $Å^{-1}$ mol^{-1}. Molecular dynamics relaxing of the optimized structures was employed to look for different possible local minima (step size of 0.001 ps, constant simulation temperature of 300 K).

Table 1
Characteristic distances in α-chitin crystal structure

Crystallographic data	Distances (nm)
(–NH as reference point in the chain)	0.301, **0.53** –NH –OH (in the same chain) and to –NH (the next chain)

The distances are determined by editing an α-chitin unit cell and taking a chemical functional group (in this case a –NH) as a central reference point (the crystallographic data of the α-chitin are from Ref. [2]). The number in bold is compared to the respective bold numbers in Table 2.

Table 2
Crystallographic parameters for α-chitin and calcite

Structure	Distances (nm)			Other data (nm)
	Unit cell	With the first neighbor atoms		
α-Chitin (Orthorhombic)	***a*=0.476**	O–O	**0.216**, 0.30	
	b=0.1028			
	***c*=0.1885**	N–O	0.292, 0.366	
Calcite crystal (Trigonal)	***a*=0.498**			Ca^{2+} polyhedra
	***c*=0.1762**	(100)		Ca–O 0.235
			Ca–O 0.235	
		(001)	Ca–C 0.321	
		(104)	C–C 0.404	

The parameters in bold are remarkably similar.

3. Results and discussion

According to XRD measurements, the extracted shrimp shell spherulites are composed of highly crystalline calcite and alpha-chitin (Fig. 1). The spherulite size is between 100 and 200 nm. The amorphous peaks at low angles (2θ of about 10° and 20° in) are explained by a long-range order in the alpha-chitin structure. As found by LVSEM, they have a very homogeneous shape (Fig. 2).

By using AFM on the samples with white spots (Fig. 3), the spherical shapes from Fig. 2 are reproduced again under higher magnification. We did not observe, however, any periodic structures even when scanning at higher resolution (data not shown). This could be explained by the calcite being enveloped with a layer of α-chitin.

In the other hand, one can see that the periodicities of radicals in the unit cell of the α-chitin (in Table 1, –NH as a central reference point) can match some of the periodical features of the calcite unit cell. As an example, in calcite the unit cell parameter *a* (in Table 2 in black, 0.498 nm) can match some of the distances among radicals in the α-chitin structure (Table 1 in black, 0.53 nm) (α-chitin crystallographic data obtained from Ref. [2]). The molecular matching between the two components in the shrimp exoskeleton led us to perform a molecular model of the hybrid ducking.

Regarding the chemical nature of the fibrous polymer (the presence of amide, hydrogen bonds and their interaction with the crystal structure), we tried to give an insight by using infrared spectroscopy for the samples with and without white spots. In the FT-IR spectra (Fig. 4), we observed first of all a

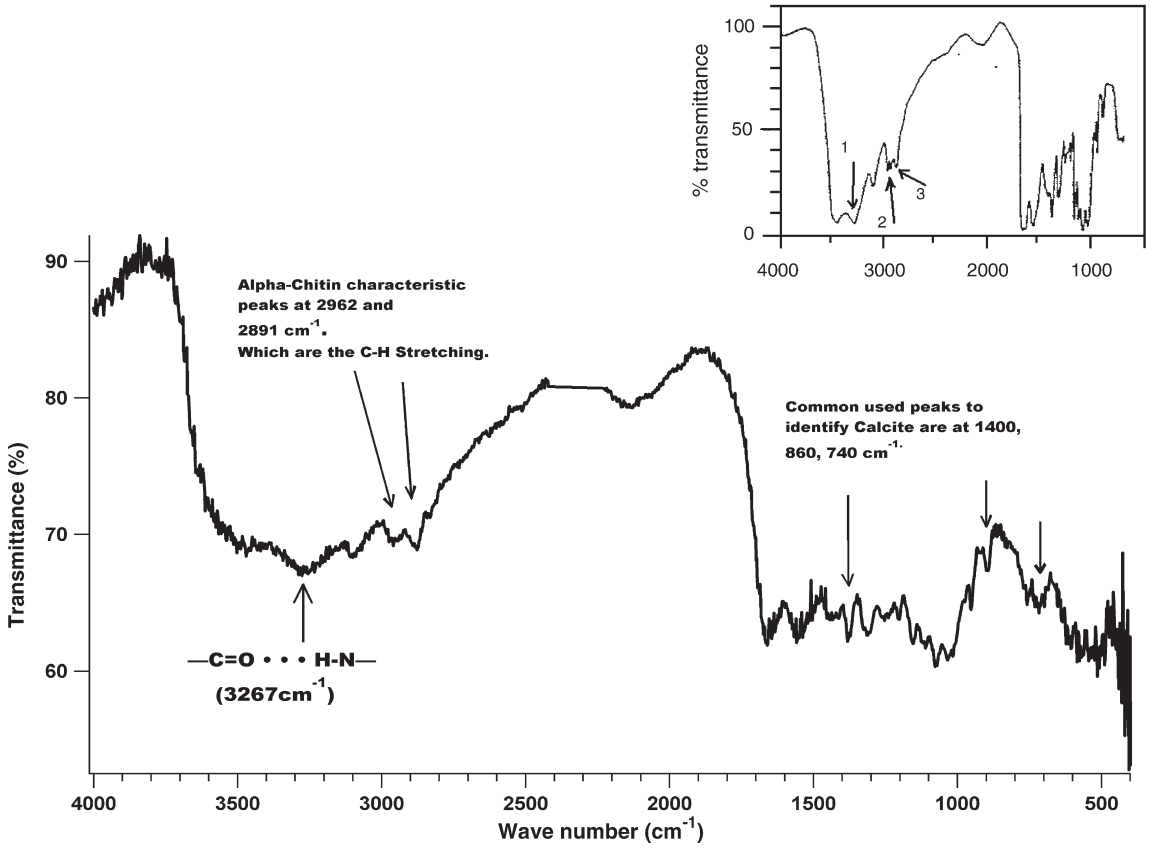

Fig. 4. FT-IR spectra for the shrimp shell samples with white spots. The peaks from α-chitin and calcite are present, with some differences as compared to pure α-chitin (peaks 1–3 in the inset, taken from Ref. [1] with permission of the publishers). Band at 3267 cm^{-1} shows a possible $–NH\cdots CO_3^{-2}$ interaction. Other interactions can be masked by the calcite bans.

series of bands related to calcite at 2523, 1800, 1451, 880 and 719 cm^{-1}, as well as the bands related to α-chitin at 3267, 2962 and 2891 cm^{-1}.

Intense bands were found at about 1655 and 1555 cm^{-1}. Both are typical for amides and correspond to stretching vibrations of carbonyl groups, including in chitins ($\nu_{C=O}$, usually called 'amide I'), and to δ_{NH} ('amide II'), respectively [1,21]. Compared to the FT-IR spectrum of pristine α-chitin [1,2,22] (inset in Fig. 4), one can see that the peaks related to amides and the CH stretching vibrations in the sample with white spots are less pronounced although it must be discussed. Other authors have also reported similar differences when this biopolymer is associated to crystals [1]. This might result from the crystal–biopolymer interaction, where the organic moieties are less ordered with respect to each other than in pristine biopolymer, but instead oriented towards the crystal surface (the 3267 cm^{-1}).

To give an insight to the possible mechanisms of interaction and inhibition of some crystal planes by the docking with macromolecules or monomers [3,12,15,20,23,24] we used MM+ molecular mechanics. By combining geometry optimization and molecular dynamics (relaxing the optimized structures) we found a number of local minima. The lowest energies for different crystal planes are presented in Table 3. The highest stability was found for (104) calcite crystal plane (group of three α-chitin trimers in parallel configuration) with an interaction energy of −22.456 kcal mol^{-1}. After this value, the next one is for the same (104) plane with perpendicular orientation of three α-chitin trimers, of −19.09 kcal mol^{-1}; then follows the value of −8.558 kcal mol^{-1} for the (001) plane. These results agree with other authors' reports, which used other macromolecules (β-chitin and lysozyme) to produce different crystal morphologies [15,23], by inhibiting rhombohedral calcite planes to form mainly spheroidal or other uncommon calcite morphologies.

In the molecular model with the lowest energy of interaction ((104) parallel with –C═O; in Table 3), the radicals –C═O and Ca^{2+}, –NH and CO_3^{2-} (left and right arrow, respectively, in Fig. 5) are very close with distances of about 0.475 and 0.456 nm, respectively. Although both sides of the plane have very strong negative charges, this structure is very stable.

Table 3
Energies of interaction of three calcite crystal planes with α-chitin model (space in blank means that those atoms are not present in the mentioned crystal plane)

Crystal face	First element from the α-chitin and the second element from the crystal plane (in kcal mol^{-1})			
	O–Ca	H–Ca	H–CO_3	O–CO_3
100			16.96	2.15
001	−8.558	30.303	17.285	20.162
104 (Parallel)			2.05	**−22.456**
104 (Perpendicular)			17, 10.38	−19.09

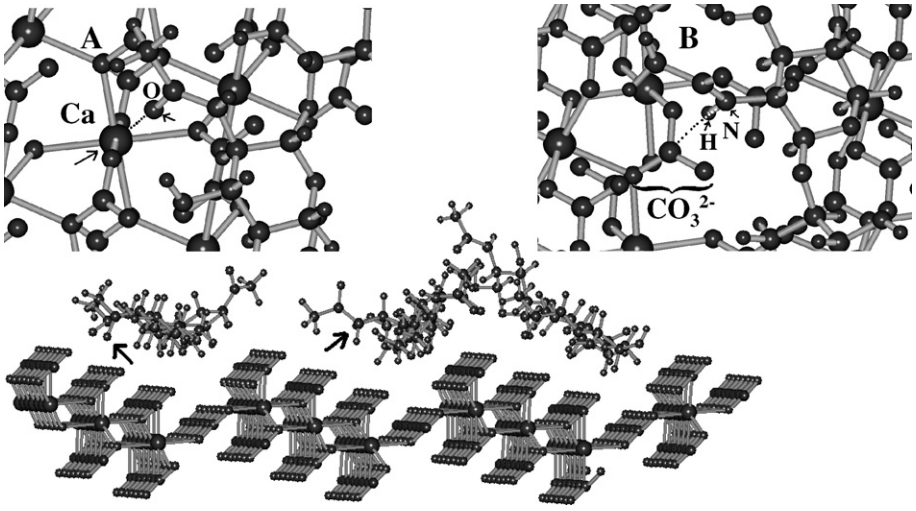

Fig. 5. Optimized geometries of the (104) crystal plane, parallel configuration, and different radicals in α-chitin trimer (MM+). The distance between O and Ca (left arrow) is 0.475 nm, and the one between NH and CO_3^{2-} (right arrow) is 0.456 nm. Amplified views are shown above: (A) oxygen atom approaching Ca; (B) NH approaching to CO_3^{2-}.

Since the charge in all models were the same, but with different orientation of α-chitin trimers, one can suggest that the geometry is a very important factor for better docking, as discussed by other authors [15,20].

4. Conclusions

The main components of spherulites from the white spot material are the α-chitin and crystalline calcite. Our theoretical results show that the (104) planes in the calcite structure are the most favored to interact with alpha-chitin, what is consistent with the experimental results [15]. AFM topography imaging suggests that the spherulites surface is covered by a layer of α-chitin.

FT-IR Band at 3267cm^{-1} (Fig. 4) reinforce the assumption that both phases have a tight contact because it shows a –NH···CO_3^{-2} interaction (Fig. 5A,B). The other interaction from our model (Ca^{2+}···O–C–) is not clear in the FT-IR study because can be masked by the normal Ca^{2+}···O from the crystal planes and not necessary from the organic–inorganic interaction.

In the other hand, the spatial orientation of CO_3^{2-} anions in (104) calcite plane can govern the three-dimensional arrangement over the biopolymer because they are inclined with respect to the crystal plane, they likely allow Ca^{+2} ions to be accessed by some functional groups of the biopolymer. The FT-IR data support our assumptions, showing wider amide I and II bands (3267, 1655 and 1555 cm^{-1}), apparently due to lowering the radical's symmetry when it bends towards the crystal surface. Thus, the CO_3^{2-} could play an important role to the nucleation of calcite when it approaches to the –NH group from the α-chitin. This work gives important information to explain the objective conditions to perform a hybrid interaction in a biological material. To our knowledge, this is the first report confirming the molecular basis of this interaction. More detailed studies and additional information are necessary on the AFM imaging, chemical and elemental composition as well as the structure of biopolymer phase, which are now under way in our laboratory.

Acknowledgements

We thank Bach. Phys. Edilberto Hernández, Sr. Pedro Mexía and Prof. Roberto Hernández for their assistance and advisory. The authors also acknowledge the financial support from CONACyT, and UNAM through the projects DGAPA-PAPIIT IN113199, IN120801, IN103700 and IN100303; and A. Heredia, DAAD Studentship.

References

[1] A. Mikkelsen, S.B. Engelsen, H.C.B. Hansen, O. Larsen, L.H. Skibsted, Journal of Crystal Growth 177 (1997) 125.
[2] A.G. Walton, J. Blackwell, Biopolymers, Academic Press, England, 1973.
[3] V.A. Basiuk, in: Martin Malstem (Ed.), Biopolymers at Interfaces, Surfactant Science Series, vol. 75, Marcel Dekker, New York, 1998.
[4] M.A. Cohen, in: Martin Malstem (Ed.), Biopolymers at Interfaces, Surfactant Science Series, vol. 75, Marcel Dekker, New York, 1998.
[5] W. Kaim, B. Schwederski, Bioinorganic Chemistry: Inorganic Elements in the Chemistry of Life. An Introduction and Guide, John Wiley & Sons Publish., United Kingdom, 1994.
[6] S. Mann, Biomineralization, Oxford University Press, United Kingdom, 2001.
[7] F. Manoli, J. Kanakis, P. Malkaj, E. Dalas, Journal of Crystal Growth 236 (2002) 363.
[8] N. Watabe, V.R. Meenakshi, P.L. Blackwelder, E.M. Kurtz, D.G. Dunkelberger, in: N. Watabe, K.M. Wilbur (Eds.), The Mechanisms of Mineralization in the Invertebrates and Plants, Belle Baruch Institute For Marine Biology and Coastal Research, University of Carolina Press, 1976.
[9] H. Wenk, A. Bulakh, Minerals. Their Constitution and Origin, Cambridge University Press, United Kingdom, 2004.
[10] E.M. Harper, Journal of Zoology, London 251 (2000) 179.
[11] Q.L. Feng, F.Z. Cui, G. Pu, R.Z. Wang, H.D. Li, Materials Science and Engineering, C 11 (2000) 19.
[12] P.R. Beena, T.K. Rao, S. Krishnamurthy, R. Vetrivel, J. Mielczarski, J.M. Cases, Langmuir 18 (2002) 932.
[13] B.R. Heywood, in: S. Mann (Ed.), Biomimetic Materials Chemistry, John Wiley & Sons Publish., 1996, p. 143.
[14] J. Lahiri, G. Xu, D. Dabbs, N. Yao, I. Aksay, J. Groves, J. Am. Chem. Soc. 119 (1997) 5449.
[15] C. Jiménez-López, A. Rodríguez-Navarro, J.M. Domínguez-Vera, Geochimica et Cosmochimica Acta 67 (9) (2003) 1667.

[16] S. Yu, H. Cölfen, J. Hartmann, M. Antonietti, Advanced Functional Materials 12 (2002) 541.
[17] E. Carrillo, H. Camarillo, J. Rubio, Physica Status Solidi, V 101 (1987) 315.
[18] A. Mikkelsen, A.B. Andersen, S.B. Engelsen, H.C.B. Hansen, O. Larsen, L.H. Skibsted, Journal of Agricultural and Food Chemistry 47 (1999) 911.
[19] L. Addadi, S. Weiner, Proceedings of the National Academy of Sciences of the United States of America 82 (1985) 4110.
[20] H. Teng, P.M. Dove, J.J. De Yoreo, Geochimica et Cosmochimica Acta 63 (17) (1999) 2507.
[21] C.T. Andrade, K.M. Silva, R.A. Simão, C. Achete, Carbohydrate Polymers 47 (2002) 59.
[22] L.J. Bellamy, The Infra-spectra of Complex Molecules, Chapman and Hall, London, 1978.
[23] G. Falini, S. Fermani, A. Ripamonti, Journal of Inorganic Biochemistry 84 (2001) 255.
[24] G. Falini, S. Fermani, A. Ripamonti, Journal of Inorganic Biochemistry 91 (3) (2002) 475.